Vol.5 No.2 April 2024

Multimedia Research

Received 4 December, Revised 10 February, Accepted 25 March

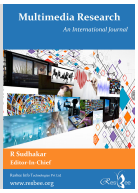

Improved Harmony Search Approach based DCNN for Image Restoration Model

Sathish Vuyyala
Assistant Professor,Computer Science & Engineering
Maturi Venkata Subba Rao Engineering College, Hyderabad, Telangana, India

Abstract: In various fields, image restoration has received huge interest and many researchers introduce several image restoration techniques to restore hidden clear images from degraded images. Moreover, aforesaid approaches performances are estimated impartially remnants the huge confront that might delay the furthermore improvement of developed image restoration techniques. Hence, an efficient noisy pixel prediction on the basis of the image restoration is introduced that uses the Deep Convolutional Neural Network (DCNN) classifier to restore the input image from several noises, such as random noise as well as impulse noise. An Improved Harmony Search Algorithm (IHSA) is adopted to train the DCNN optimally based on minimum error. After identifying the noisy pixels, by exploiting the neuro-fuzzy system the enhancement of pixel is performed. Finally, the experimental analysis is performed and the image restoration performance on the basis of IHSA is analyzed based on the SDME, PSNR, and SSIM. Ultimately, the adopted model attains the maximum PSNR SSIM for images with random noise, as well as maximum SDME with impulse noise, correspondingly.

Keywords: Hidden Image, Image Restoration, Impulse Noise, Noisy Pixel Prediction, Random Noise.

Nomenclature

Abbreviations	Descriptions
IR	Image Restoration
LR	Low-Resolution
LQ	Low-Quality
HR	High-Resolution
SSIM	Structural Similarity
HQ	High-Quality
RBF	Radial Basis Function
SRB	Sparse Residual Block
IHSA	Improved Harmony Search Algorithm
OSA	Optical Sparse Aperture
LRIRCNet	Low-Resolution Image restoration Classifier Network
MTF	Mid-frequency Modulation Transfer Function
PSNR	Peak Signal-To-Noise Ratio
SISR	Single Image Super-Resolution
BPNN	Back Propagation neural network
FC	Fully Connected
DTN	Dual Target Network
GANs	Generative Adversarial Networks
TSSN	Two-Stream Sparse Network
OITD	Online Insect Trapping Device

1. Introduction

In computer vision, IR is a significant approach that is extensively used in numerous fields namely satellite imaging, medical imaging, security monitoring, and so on. From the degraded LQ image to generate an HQ image, the IR is exploited which is usually an ill-posed issue since degradation is a permanent procedure. In order to resolve this issue, numerous techniques were presented for three classic IR tasks namely image denoising, SISR, as well as JPEG deblocking. Amongst these tasks, from LR image the SISR aspires to reconstruct HR image, from the noisy image the image denoising is to

https://doi.org/10.46253/j.mr.v5i2.a2

eliminate noise that is "usually additive white Gaussian noise with a standard deviation, as well as using the compression process of JPEG, JPEG deblocking is to eliminate blocking artifact occurred" [1].

In Image processing, noisy image restoration is considered a significant issue. So far, several IR techniques were presented such as the Low pass filter, Wiener filter, and median filter. In this filter, the Wiener filter is modeled by reducing the mean square error among the original and restored images is almost certainly well-liked, however, the standard Wiener 1lter degrades significant edge information because of its low-pass filtering natures. For the resolution, various non-stationary filters which can alter the filter characteristics consistent with local image characteristics were presented in many works. To remove impulsive noise, the median filter is helpful and the low-pass fi1ter is computationally effectual, other than they show deprived restoration performance than Wiener fi1lter in least-squares mean. Nevertheless, the sparse arrangement occurs the MTF is very much attenuated. Hence, because of noise and the attenuated MTF, the captured raw image is a rigorously degraded version. IR model is necessary to obtain a clear and high-contrast image. General signs to evaluate the effect of image restoration include SSIM, PSNR, and mid-frequency contrast. The SSIM and PSNR can be attained via easy computations while the ideal image is recognized. "The mid-frequency contrast change can be seen in the Fourier domain" [2].

Even though the conventional IR technique is easy and effective it has aspired at easy image denoising [3]. In general, image degradation is a multifaceted procedure, as well as restoration techniques, are hardly ever exploited in practice. When the likelihood probability of an image is known from a Bayesian point of perspective, image prior probability will play an important role in IR outcomes. Numerous techniques were modeled to obtain prior knowledge of images, such as the gradient descent technique, sparse technique, non-local self-similarity technique, and Markov random field technique [4].

The main aim of this work is to present an Improved Harmony Search algorithm (IHSA) for image restoration. Here, the adopted model performs in two stages. In the first stage, the pixel map is produced and then noisy pixel is identified and finally, the pixel enhancement is performed. Initially, from an input image, generation of noisy pixel map is carried out, and subsequently based on DCNN the noisy pixels are recognized and that is trained using the adopted IHSA model. Finally, the enhancement of pixels is performed based on the fuzzy neuro system.

2. Literature Review

In 2020, Mei Hui *et al., [*1], worked on a DTN for the IR of OSA systems. The noise was calculated with interpolation and difference computation in a raw image. A denoiser is exploited for the block matching 3D filter. A denoised image was considered a degraded image that cannot be precisely modeled. A dual-target such as negative structural similarity as well as a summation of fidelity as well as regularization term network was trained to handle the restoration issue. Using the filling factor, a function was ascertained as well as aperture distribution was trained as an alteration network term. To deconvolve the denoised image, a trained network was exploited. In 2020, Shuhui Wang *et al.,* [2], presented a TSSN to openly learn shallow as well as deep features to put into effect their own contribution to IR. The shallow features for instance texture edges, as well as deep stream, learn deep features, for instance, salient semantics was learned by the shallow stream. SRB was presented for each stream, to competently collective hierarchical features by constructing sparse links amid layers in the local block. To combine the shallow and deep streams the channel-wise and spatial-wise attention was exploited. In 2019, Hongzhi Xue and Hongwei Cui [3], worked on information transmission technology as well as computer technology development, information acquisition model was chiefly transformed from character to image at present. Nevertheless, image damage and quality minimize because of the several factors in the obtaining and transmitting images process. Hence, in the image processing field, how to restore an image has turned out to be a research hotspot. This work introduces an image restoration technique on basis of BPNN. In 2019, Huiling Zhou *et al.,* [4], worked on the sticky board traps that were extensively exploited to capture insects in warehouses or grain bins and their backgrounds. Here, an OITD was modeled and developed by the group; it was exploited to routinely obtain the insect's images detained on sticky boards. To enhance the recognition high-noise as well as low-resolution insect images performance was captured by OITD. Here, an LRIRCNet on the basis of GANs was proposed and estimated for its performance. In 2003, Kaoru Inoue *et al.,* [5], worked on a reduction of noise filter which can reduce noise modules without obliterating significant image information. To get better a high-quality image from a tarnished version, the RBF network was subsequently exploited. Based on the local image characteristics, the regularization parameter was adjusted. A rapid technique to compute the RBF network with variable regularization parameters was proposed using the Kronecker product properties.

3. Proposed Image Restoration Model

This paper presents a novel technique named IHSA based DCNN approach is developed for image restoration. Initially, the input image is subjected to the noisy pixel generation phase, wherein generation of noisy pixel map effectually takes place. To the noisy pixel recognition phase, the produced noisy pixel map is given wherein noisy pixels are recognized on the basis of the DCNN classifier that is optimally trained using the optimization approach. At last, recognized noisy pixels are transmitted to pixel phase improvement, wherein pixel enhancement is performed by exploiting the neuro-fuzzy system. Fig. 1 shows a block diagram of the adopted technique for image restoration.

Let us consider the J as input image J with size $U \times V$, as well as input image pixel position is indicated as $J(l,m)$. Because of noise attend in image; definite element of the image is tainted as well as residual pixels are taken into consideration as noise-free. The recognized noise pixels are highly confronting therefore, the DCNN model is exploited in this work to recognize the noisy pixels by taking into consideration of the image neighborhood. Here, for the identification of the pixel, the DCNN is exploited. For image pixels, to generate the prediction map the DCNN is exploited. On the basis of the input image, the DCNN classifier [6] produces the prediction map.

3.1 DCNN Model

DCNN [6] is discussed in this section and it consists of the number of pooling layers (POOL), FC layers as well as convolutional (Conv) layers. Each layer comprises a specific function amid three layers of DCNN. The important function of Conv layers is to produce feature maps from pre-processed image segments. Furthermore, in the pool layers, aforesaid feature maps are sub-sampled down. In the FC layer, the classification process takes place. To model the output map, the convolutional layer produces in mapping input so that input maps experience convolution with convolutional kernels. The output map size is similar to kernel number as well as kernel matrix size is $[3 \times 3]$. Therefore, the conv layers are kernel weights, input maps multilayer loop, as well as output maps. In the initial Conv layer, there is a number of inputs and outputs, and its size minimizes in consecutive Conv layers so that the classification accurateness of objects based upon the number of layers in DCNN.

Conv layers: To extract a feature convolutional layer is used and presents the pattern extraction by exploiting the feature vector attained from the input image. By exploiting trainable weights the neurons are connected and "these trained weights are convoluted by means of inputs to model feature maps. Subsequently, the result is fed to the non-linear activation function to easiness complex functional mappings amid the input as well as response variables" [6]. Consider, G as input to deep CNN as well as therefore, the outcome from the convolutional layer is stated as below:

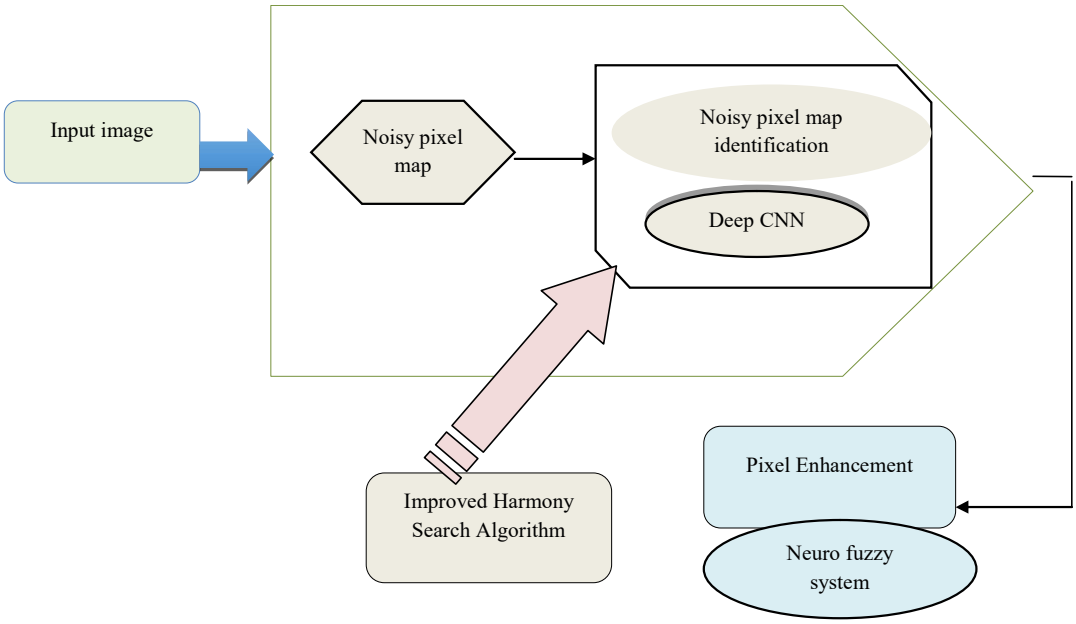

Fig.1. *Architectural model of adopted technique for image restoration*

$$(M_c^b)_{i,j} = \left(B_c^b\right)_{i,j} + \sum_{d=1}^{\varpi_I^{d-1}} \sum_{k=-\varpi_1^l}^{\varpi_1^l} \sum_{n=-\varpi_1^l}^{\varpi_2^l} \left(\vartheta_{c,d}^b\right)_{k,n} * (J)_{i+k,j+n} \quad (1)$$

wherein, $\left(B_c^b\right)_{i,j}$ defines fixed feature maps, $*$ defines convolutional operator that set up pattern extraction from outputs attained from neighboring convolutional layers. The output from the preceding $(b-1)^{th}$ layer creates input to 1^{th} convolutional layer. $\vartheta_{c,d}^b$ represents the weight of convolutional layer, that is the weights of b^{th} convolutional layer as well as B_c^b bias of b^{th} convolutional layer. Assume d, k, and n represents the feature maps notations.

ReLU layer represents activation function to ensure the efficiency and easiness, as well as the ReLU layer importance, is which the DCNN with ReLU works quicker to deal with the huge networks. From the ReLU layer the output while subjected to the feature maps is stated as follows:

$$G_c^b = Afn\left(M_c^{b-1}\right) \quad (2)$$

wherein, $Afun(\ )$ indicates activation function in b^{th} layer.

POOL layers are non-parametric layers with no bias as well as weights experiencing a fixed operation. Moreover, this layer's significance is to alleviate input spatial dimensions and reduce computational complexity.

FC layers: By exploiting the convolutional as well as pooling layers the patterns are created and form input to fully-linked layers which are fed to maximum-level analysis. The following equation states the output from the fully linked layers,

$$H_c^b = \delta\left(G_c^{b-1}\right) \text{ with } M_c^b = \sum_{d=1}^{\varpi_I^{d-1}} \sum_{k=-\varpi_1^l}^{\varpi_1^l} \sum_{n=-\varpi_1^l}^{\varpi_2^l} \left(\vartheta_{c,d}^l\right)_{k,n} * (J)_{i+k,j+n} \quad (3)$$

wherein, $\left(\vartheta_{c,d}^l\right)_{k,n}$ indicates weight.

3.2 Statistical Model for the Noisy Pixel Restoration

Subsequent to the noisy pixel recognition, for equivalent noise pixels, the novel pixel values are calculated. By exploiting the following formulation, the noisy pixel is eradicated while the noisy center pixel is recognized.

$$J_{np}(l,m) = \begin{Bmatrix} J_n(l,m) & \text{if } M(x,y)=1 \\ J(l,m) & \text{otherwise} \end{Bmatrix} \quad (4)$$

wherein, $J_n(l,m)$ indicates a new pixel image value. The chosen noisy pixel is merely appropriate for calculating new pixel values. Initially, 3×3 window $J(u,v)$ is produced, as well as subsequently matching is performed with a noisy pixel of 3×3 window $J(u,v)$ as well as the input image $J(l,m)$. The similarly matched pixels N_S are taken into consideration for further processing from the matching output. The value of the novel pixel is generated or noisy pixels are altered using a raw image in chosen 3×3 windows while N_S is superior to the threshold value T_l. T_l value is taken into consideration as 21. Moreover, new pixel values are calculated on the basis of the L_b, Z, and B parameters, which is stated as follows:

$$E(l,m) = e(L_b, Z, B) \quad (5)$$

wherein, Z indicates the absolute function of 3×3 window on basis of the neighbour pixel which is represented as follows:

$$Z = abs(J(u,v) - J(u+x-3, v+y-3)) \quad (6)$$

With prefixed window L_b value is derived using the absolute output of eq. (6). Initially, L_b value is set to "0" in that b varies based on the chosen prefixed window.

$$L_b = L_b + Q_l(l,b) * Z; 1 \le b \le \omega \quad (7)$$

For X_b rounding process is performed as well as it is round by $\frac{L_b}{8}$ that is indicated as g. After the rounding, the sorting process is performed for the outcome attained from L_b wherein the first value is chosen E.

$$E(l,m) = \begin{Bmatrix} 1 - (E-1)/4 & E > 10 \\ 1 & \text{otherwise} \end{Bmatrix} \quad (8)$$

Eq. (8) outcome is compared with T_2 and the value is set to 0.2. While $E(l,m)$ the value is superior to the second threshold value, the function is generated.

$$RP(l,m)=\begin{Bmatrix} sum(P\alpha)/q_1 & s > T_3 \\ E(l,m) & otherwise \end{Bmatrix} \tag{9}$$

wherein, q_1 indicates constant in that the q_1 value is set to 4 and α indicates mean value of neighborhood pixel. The following formulation indicates the evaluation of the mean value,

$$\alpha = e^{\left(Y_a * Y_a / 0.001+2\beta^2\right)} \tag{10}$$

wherein, β indicates standard deviation. While the outcome attained from eq. (9) is evaluated with a threshold value T_3 . Moreover, T_3 value is fixed to 23. If it is superior to the T_3 the new pixel value is produced by exploiting the formulation as stated as follows:

$$J_n(l,m)=\frac{EP_A}{EP_B}=\frac{\sum(J(l,m).M(l,m))}{\sum M(l,m)} \tag{11}$$

3.3 Neuro-fuzzy System for Image Enhancement

Subsequent to the new pixels recognition, the enhancement of the image process is carried out on basis of the neuro-fuzzy system. The image enhancement presents detailed information regarding the boundaries, edges by means of increased dynamic range. Moreover, an improvement procedure is performed on basis of noisy pixels. If noisy pixels position K is recognized then the recognized pixels are used for the improvement procedure. Subsequent to, the new image matrix is produced on basis of nearest neighbor for the noisy pixel is indicated as follows:

$$\underset{\forall K}{J_{n1}(l,m)}=\frac{1}{9}\sum_{u=1}^{1}\sum_{v=1}^{1}J_n(l+u,m+v) \tag{12}$$

To resolve the uncertainty problems, the produced new pixel values are fed to the neuro fuzzy system.

$$\underset{\forall K}{J_{n2}(l,m)}=N_{fuzzy}(J_n(l,m)) \tag{13}$$

wherein, N_{fuzzy} indicates neuro-fuzzy system. If a neuro fuzzy set approach is produced, a new pixel $J_n(l,m)$ is taken into consideration as input as well as a new image is produced by exploiting noise pixel-based position. Finally, restored image is attained from the following formulation:

$$\underset{\forall K}{J_G(l,m)}=\left[\frac{\underset{\forall K}{J_{n1}(l,m)}+\underset{\forall K}{J_{n2}(l,m)}}{2}\right] \tag{14}$$

The ANFIS structure [7] consists of outcome and basis kinds. To determine the parameters associated with the parts, ANFIS is trained used in the optimization algorithm. In the training, the ANFIS exploits the input as well as output data pairs. In ANFIS layers in attendance are normalization, defuzzification, fuzzification rule, as well as summation layer. Moreover, membership functions are exploited by the fuzzification layer to attain the fuzzy clusters from input values wherein firing strengths are generated on basis of the membership values estimated in fuzzification, where to calculate firing strengths similar to each rule normalization layer is used. The normalized value indicates the ratio of firing strength to i^{th} rule to the total amount of firing strengths. For each node, the defuzzification layer calculates weighted values when the summation layer added outcomes attained from the defuzzification layer.

4. Proposed Model

The HSA has been effectively used in Image Restoration [8]. The easy mathematical model enables its improved implementation to address engineering problems compared to numerous other bio-inspired methods.

The harmony vectors are generated using the eq. (15) and (16).

$$Z_i=(z_i(1),z_i(2),.....z_i(n)) \tag{15}$$

$$z_i=lb(j)+(ub(j)-lb(j))\times rn(0,1) \tag{16}$$

wherein $rn(0,1)$ indicates an arbitrary number subsequent to a uniform distribution of (0, 1). Then the Harmony is constructed by exploiting the Harmony vectors as well as their fitness function values $f(Z_i)$

$$HM = \begin{bmatrix} Z_1 & f(Z_1) \\ Z_2 & f(Z_2) \\ \vdots & \vdots \\ Z_{HMS} & f(Z_{HMS}) \end{bmatrix} = \begin{bmatrix} z_1(1) & z_2(1)\ldots & z_1(k) & f(Z_1) \\ z_2(1) & z_2(1)\ldots & z_2(1) & f(Z_2) \\ \vdots & \vdots\ \ldots & \vdots & \vdots \\ Z_{HMS}(1) & Z_{HMS}(2)\ldots & Z_{HMS}(k) & f(Z_{HMS}) \end{bmatrix} z_1(1) \quad (17)$$

The random value r is generated and it follows the uniform distribution of (0,1)

The bias factor is set as $0 < \beta < 0.5$ that stands for the exploration direction probability. With β, then update Z_i by a step towards *UB*. Meanwhile, with the probability of 1- β, then Z_i is updated a step towards *LB*. The exploration principles for updated vector Z_i^{new} are devised as:

$$Z_i^{new} = \begin{cases} Z_i + r * BW, & r \le \beta \\ Z_i - r * BW, & r > \beta \end{cases} \quad (18)$$

4.1 Harmony Search is Updated using Levy Flight

Numerous bio-inspired techniques have inadequate searching capability because of the limited iteration time, when using the Levy flight model might aid increase the effectual searching range, augment population diversity, as well as therefore evade local optimum. The most important Levy flight feature is to enhance behaviors of the arbitrary or stochastic walk, thus it has the ability to choose a fixed or arbitrary step to update Harmony vector.

Generate vector X_i arbitrarily in the allowable area to Harmony, as well as set $m = 1$.

Update the Harmony vector Z_i^{new} by exploiting the Levy flight:

$$Z_i^{new} = Z_i + \lambda \cdot levy(d) \quad (19)$$

wherein λ represents the walk step, as well as d represents location vectors dimension for Levy flight. The arbitrary searching path $levy(d)$ is computed as:

$$levy(d) = 0.01u \cdot \phi / |v|^{\frac{1}{\gamma}} \quad (20)$$

where, u and v indicates two arbitrary numbers in (0,1) ; γ represents a constant, and ϕ represents computed as:

$$\phi = \left\{ \frac{\Gamma(1+\gamma) \times \sin\left(\pi \times \frac{\gamma}{2}\right)}{\Gamma\left\{\left[\left(\frac{1+\gamma}{2}\right)\right] \times \gamma \times 2^{\frac{\gamma-1}{2}}\right\}} \right\} \quad (21)$$

wherein $\Gamma(x) = (x-1)!$. The constraint for X_i^{new} is *LB UB*.

In the proposed algorithm, setting $0 < \beta < 0.5$ can reduce redundant exploration to an enormous degree, as well as accelerate searching speed without failing global searching area.

Then by using levy flight improved stochastic behavior, randomness, as well as exploration capability, however, it might consume more time. Auspiciously, Step 6 by adding the bias factor restores searching time to few degree, hence searching capability, as well as speed, can be well balanced.

5. Result and Discussion

In this section, the results attained using the adopted IHSA-based DCNN model were shown and the performance was validated on the basis of the SDME, PSNR, and SSIM. Here, the proposed method was compared with the conventional models such as NN [9], KNN, CNN, SVM, Deep CNN, and ANN [10].

Fig. 2 and 3 represent the performance analysis of the adopted technique and the conventional techniques regarding impulse noise as well as random noise. Here, PSNR and SDME are attained by the proposed and conventional techniques with random and impulse noise by varying noise levels. It is clearly indicated that the adopted model has obtained superior performance with random noise by deviating noise levels.

Fig. 4 demonstrates performance analysis of the adopted technique and the conventional techniques regarding SSIM for impulse noise as well as random noise. The SDME attained by the proposed technique attained better SSIM. Here, the proposed method is 15% better than the NN, 21% better than the KNN, 23% better than the CNN, 25% better than the SVM, 18% better than the Deep CNN, and 12% better than the ANN with impulse noise .

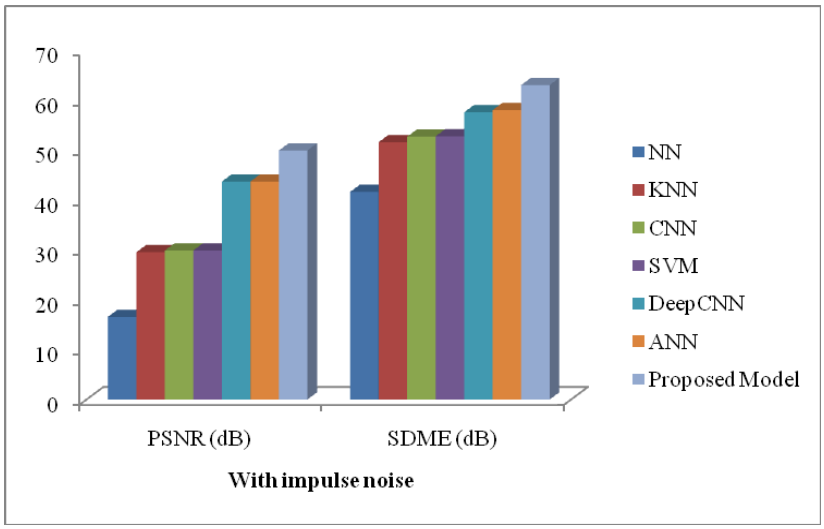

Fig.2. Performance analysis of the adopted technique and the conventional techniques regarding impulse noise

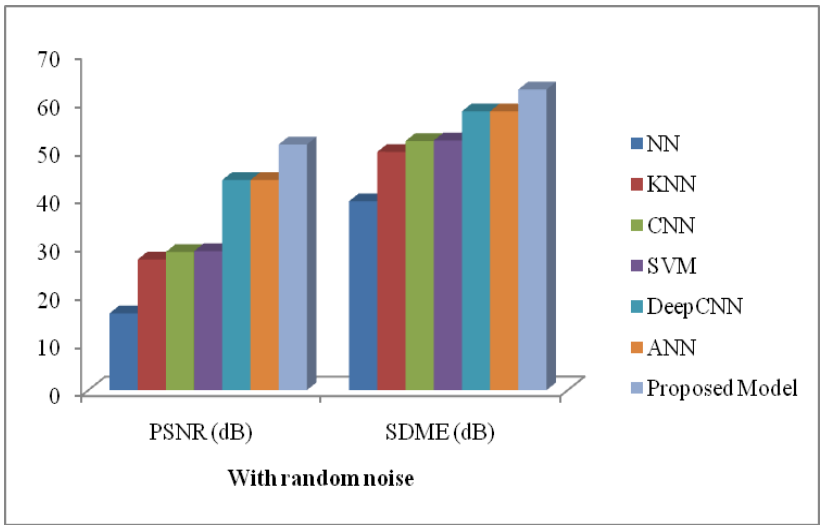

Fig.3. Performance analysis of the adopted technique and the conventional techniques regarding random noise

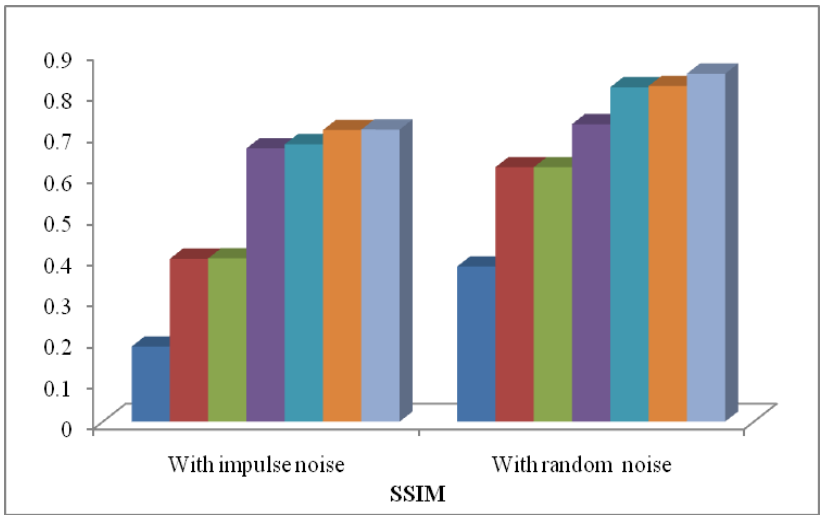

Fig.4. Performance analysis of the adopted technique and the conventional techniques regarding SSIM

6. Conclusion

In this work, the image restoration technique on the basis of the IHSA based DCNN model was presented. It was exploited to restore input images from the random noise as well as impulse noise. Moreover, the image restoration process was carried out using three phases. Initially, the DCNN was developed to recognize noisy pixels from the input image. Then, in the second stage on basis of IHSA, the identified noisy pixels will eradicate. Finally, the adopted neuro-fuzzy system was exploited for the enhancement of the pixels. Hence, the adopted technique restores the image by eradicating various kinds of noises such as impulse as well as random noise. At last, the performance analysis was performed using the adopted optimization algorithm regarding the SDME, PSNR, and SSIM. The adopted technique achieves maximum SSIM, PSNR, and SSIM which shows the betterment of the adopted technique.

Compliance with Ethical Standards

Conflicts of interest: Authors declared that they have no conflict of interest.

Human participants: The conducted research follows the ethical standards and the authors ensured that they have not conducted any studies with human participants or animals.

Reference

[1] Mei HuiXinji LiYuejin Zhao,"Image restoration of optical sparse aperture systems based on a dual target network", Results in Physics, 25 September 2020.
[2] Shuhui WangLing HuQingming Huang,"Two-stream deep sparse network for accurate and efficient image restoration", Computer Vision and Image Understanding, 29 June 2020.
[3] Hongzhi XueHongwei Cui,"Research on image restoration algorithms based on BP neural ", Journal of Visual Communication and Image Representation, 11 January 2019.
[4] Huiling ZhouHaiwei MiaoDigvir S. Jayas,"A low-resolution image restoration classifier network to identify stored-grain insects from images of sticky boards", Computers and Electronics in Agriculture, 9 May 2019.
[5] Kaoru InoueYouji IiguniHajime Maeda," Image restoration using the RBF network with variable regularization parameters", NeurocomputingJanuary 2003.
[6] Kai Zhang, WangmengZuo, Shuhang Gu, and Lei Zhang, "Learning Deep CNN Denoiser Prior for Image Restoration," Computer Vision and Pattern Recognition, pp. 1-10, 2017.
[7] DervisKaraboga, and Ebubekir Kaya, "Adaptive network based fuzzy inference system (ANFIS) training approaches: a comprehensive survey", Artificial Intelligence Review, vol.52, no.4, pp.2263-2293, 2019.
[8] P. Li, R. Li, Y. Cao, D. Li and G. Xie, "Multiobjective Sizing Optimization for Island Microgrids Using a Triangular Aggregation Model and the Levy-Harmony Algorithm," in IEEE Transactions on Industrial Informatics, vol. 14, no. 8, pp. 3495-3505, Aug. 2018.
[9] Nisha Malik,"Rainfall prediction using Back Propagation Neural Network Model with Improved Flower Pollination Optimization Algorithm", Multimedia Research, vol. 3, no. 3, July 2020.
[10] Ganeshan R,"Skin Cancer Detection with Optimized Neural Network via Hybrid Algorithm", Multimedia Research, vol. 3, no. 2, April 2020.